Open access • Proceedings Article • DOI:10.1117/12.339890

Pulse phase thermography for defect detection and visualization — Source link

Sergio Marinetti, Yuri A. Plotnikov, William P. Winfree, Alberto Braggiotti

Institutions: Langley Research Center

Published on: 28 Jan 1999

Topics: Thermography

Pulse phase thermography for defect detection and visualization

Sergio Marinetti[1], Yuri A. Plotnikov[2], William P. Winfree[2], and Alberto Braggiotti[3]

[1]Consiglio Nazionale delle Ricerche - ITEF, Corso Stati Uniti, 4, 35127, Padova, Italy

[2]NASA Langley Research Center MS 231, NASA Langley Research Center, Hampton, VA 23681-0001

[3]Consiglio Nazionale delle Ricerche - LADSEB, Corso Stati Uniti, 4, 35127, Padova, Italy.

ABSTRACT

Pulse Phase Thermography (PPT) has been reported as a novel powerful technique of the thermal NDE. It employs application of the Discrete Fourier Transform (DFT) to thermal images obtained following flash heating of the front surface of a specimen. The computed phasegrams are excellent for defect visualization in a wide range of materials. This is in part due to their low sensitivity to uneven heating. This work is an attempt to analyze advantages and limitations of PPT. Results of application of the DFT to simulated temperature decays are presented. The temperature evolution on a surface has been simulated based on an analytical solution of the one-dimensional heat diffusion problem. A more sophisticated study has been done for different sizes of defects using numerical solution of the three-dimensional mathematical model. Capabilities of PPT for in-depth scanning and for monitoring of the material loss are discussed. The recommendations for the practical application of the PPT are presented. Experimental results obtained following these recommendations are reported.

Keywords: transient thermography, Discrete Fourier Transform, image processing, phase contrast.

1. INTRODUCTION

Pulse Phase Thermography (PPT) has been introduced as a new technique that combines together the advantages of Modulated Thermography (MT) and Pulsed Thermography (PT)[1]. For MT a single frequency is launched into the specimen and analyzed in the stationary regime, while for PT the responses to all the frequencies are incorporated into a single transient signal. PPT uses the experimental procedure from PT and the data analysis technique from MT. It is based on the Discrete Fourier Transform (DFT) of sampled thermal decay $T(t)$ following the pulse stimulation. The output is represented by a function of the phase.

PPT has been applied to many different kinds of material (Nylon®, metals, CFRP, plastic, plaster, wood, etc.)[2,3] with promising results. For most cases PPT showed better results than traditional amplitude and time analysis. Nevertheless, it requires a careful choice of DFT parameters. It has been noticed that, for applications to sequences suited to classical time analysis, PPT performances are not as good as expected. For example, defects may be barely visible in the phase image, while they can be easily detected in the transient thermal images. Also defects of the same nature located at different depths sometimes appear with a negative phase shift with respect to the sound area and sometimes with a positive one, etc.

Therefore, PPT needs to be further investigated in order make it a reliable technique. The purpose of this work is to provide the end-user with practical recommendations for implementation of PPT. Hence, this paper does not discuss the characterization of flaws from the phase shift (inverse problem), rather it will suggest how to acquire the thermal signal in order to ensure the reliability of its frequency representation.

2. RELEVANT PROPERTIES OF THE DISCRETE FOURIER TRANSFORM (DFT)

The Fourier representation of a function is a superimposition of sines and cosines[4]. The Fourier Transform (FT) maps a function in the time domain into a function in the frequency domain. The frequency content of the signal can then be analyzed since the Fourier coefficients of the transformed function represent the contribution of each sine and cosine function at each frequency. Let $T(t)$ be a real sequence, then the magnitude and the real part of its FT $\theta(f)$ are even functions while the phase and the imaginary part are odd functions. For all the following considerations, $T(t)$ is assumed to be a real function.

Sampling a continuous signal at the rate t_s (thus obtaining a discrete signal) limits the frequency domain to a maximum frequency $f=(2t_s)^{-1}$. If a discrete signal has a finite number of samples N, it is possible to introduce an alternative Fourier representation called Discrete Fourier Transform (DFT) that is discrete, periodic and has periodicity corresponding to N equally spaced frequencies of the FT in the frequency interval $[-f, f]$. Sampling a continuous signal and considering a finite number of samples introduces two important concepts: the frequency resolution and the aliasing.

Frequency resolution is important when the required information is a function of the event frequency or when a very narrow range of frequencies is to be studied. A coarse frequency resolution groups together contributions from different components into a single frequency, making it difficult to resolve information about each component. Therefore, the frequency resolution needs to be fine enough to enable discrimination of each signal of interest. Frequency resolution depends on the acquisition duration (i.e. if the acquisition time is $N \cdot t_s$ seconds, the frequency resolution is $(N \cdot t_s)^{-1}$ [Hz]).

An aliasing error arises when the sampling frequency $f_s=t_s^{-1}$ is lower than the bandwidth $2 \cdot B$ of the signal (where B is the bandwidth of the positive part of the spectrum). It is due to the fact that all the spectrum components at frequencies greater than $f_s/2$ introduce a contribution in the band $[0, f_s/2]$. For signals with unlimited bandwidth, it is sometimes possible to find a value of B such that all the components at frequencies greater than B can be considered negligible thus keeping the aliasing error below a certain level (signals with an "*in practice*" limited bandwidth).

3. PULSED INFRARED THERMOGRAPHY SIGNALS AND ACQUISITION PARAMETERS

In a PT experiment, data are obtained by heating the sample with a pulse stimulus and observing the temperature decay $T(t)$ on the same surface. For a time domain analysis the acquisition parameters (i.e. sampling rate and observation time) are directly deduced from the signal of interest. For instance, if the maximum temperature difference ΔT between defective and sound areas is to be analyzed, the sampling rate should be high enough to capture the maximum signal of the shallowest defect and the observation time should be long enough to capture the maximum of the deepest defect. While this acquisition procedure is correct in the time domain, in the frequency domain it provides results that are inadequate.

Consider the 1D analytical solution of the Fourier equation for the cooling stage of a plate of thickness L $[m]$ and thermal diffusivity α $[m^2s^{-1}]$ heated with a square pulse of power density Q $[Wm^{-2}]$ and duration t_h $[s]$ (in this case t_h is short enough to consider the stimulus as an instantaneous pulse):

$$T(t) = \frac{Q}{h} \sum_{n=1}^{\infty} \frac{2Bi}{Bi(Bi+1)+\mu_n^2} e^{-\mu_n^2 Fo} \left(e^{\mu_n^2 Fo_h} - 1 \right), \tag{1}$$

where h is the surface heat exchange coefficient $[Wm^{-2}K^{-1}]$, Bi the Biot Number, μ_n the positive roots of the equation $\mu \cdot tan(\mu)=Bi$, Fo and Fo_h respectively the Fourier number for t and t_h. The analytical expression of the Fourier transform of eq. *(1)* is

$$\theta(f) = \frac{Q}{h} \sum_{n=1}^{\infty} \frac{2Bi}{Bi(Bi+1)+\mu_n^2} \left(1 - e^{-\mu_n^2 Fo_h} \right) \frac{e^{-j2\pi f t_h}}{\left(\mu_n^2 \alpha \right) / L^2 + j2\pi f}. \tag{2}$$

In Fig. 1a (that is referred to a CFRP sample with $\alpha=4 \cdot 10^{-7}$ m^2s^{-1}, $L=20$ mm, $K=0.64$ $Wm^{-1}K^{-1}$ considered as a reference) the magnitude profile of eq. *(2)* (solid line) is reported. It is clear that the bandwidth of the spectrum is infinity; therefore, sampling the signal will introduce aliasing errors. The same figure shows how the same spectrum is distorted for too short experiment duration and too low sampling rate. In the first case, in addition to a poor frequency resolution, it can be observed that the first samples (0 Hz and 0.014 Hz) appreciably differ from the analytical solution due to truncation error. Only higher frequencies are well represented. In the second case the frequency resolution is greater with the very low frequencies being well represented. However, the higher frequencies are strongly affected by aliasing error. Hence, to properly choose the acquisition parameters, the frequency range of interest must be identified.

A typical output of PPT algorithm is an image with each pixel representing the phase at a fixed frequency. Hence, defect

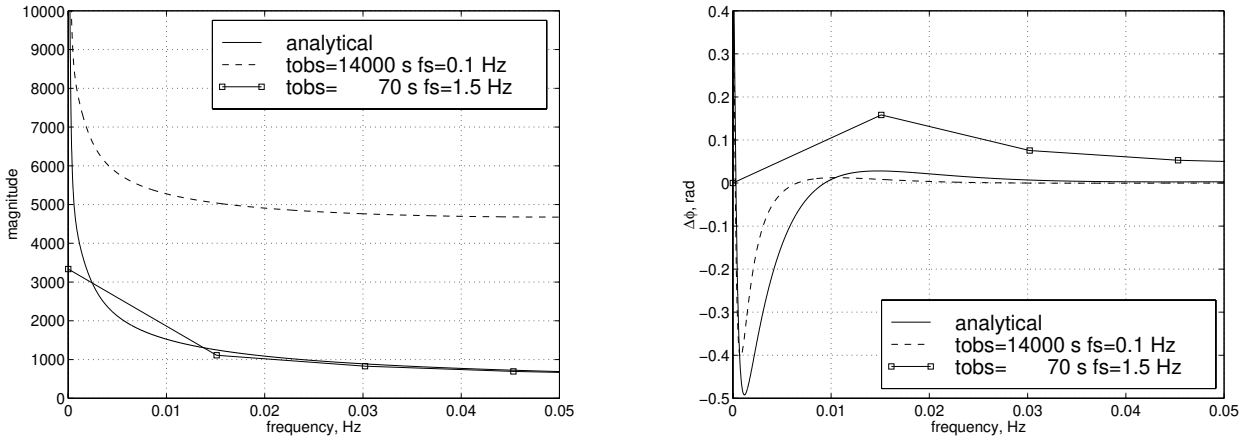

(a) *(b)*

Figure 1. Amplitude (a) and phase difference (b) of the simulated thermal profile.

visibility is a function of the phase difference, $\Delta\phi$, between a reference point and a defect. Therefore, considering the phase difference as the informative parameter, more specifically of interest is the maximum absolute value that gives the best signal to noise ratio.

Considering another sample with the same properties as the previous one but 6 mm thick, Fig. 1b shows the profile of the $\Delta\phi$ between a 20 mm thick sample (sound material) and a thinner one (defect). The maximum phase shift occurs at around 0.001 Hz. Therefore, to resolve this frequency, the signal has to be observed at least for 1000 s. As seen in Fig. 1b, the first frequency resolved with an observation interval of 70 s is at 0.014 Hz. Moreover, $\Delta\phi$ is positive and lower than expected. In contrast, a duration of 14000 s ensures an acceptable shape and resolution; however, the low sampling rate does not allow to reach the maximum value of $\Delta\phi$.

4. DURATION

Signal duration t_{obs} (i.e. observation interval) is essential in DFT because it defines the frequency resolution of the phase spectrum through the equation:

$$\Delta f = \frac{1}{t_{obs}}. \tag{3}$$

t_{obs} must be at least as long as the period of the lowest desired frequency contained in the thermal response to ensure proper resolution. The main problem then becomes: what is the lowest frequency contained in the signal which has to be resolved? This frequency determines the minimum observation interval required for the measurement.

For PPT, the captured signals represent surface temperature decays. A direct approach would be to follow traditional rules of the sampling theory (which is essentially an inversion problem without consideration of a reference point selection).

For this case, the interest is detecting and visualizing the defects. The needed information will therefore be contained in the interval where defect temperature signal differs from sound zone signal and at least this interval should fall entirely in the acquisition duration. Practically speaking, this interval is represented by the duration of the thermal contrast. For the sake of simplicity, from now on $\Delta T = T_{defect} - T_{sound}$ will be considered.

The simulated defected and non-defected area signals and the moments where the signals have been truncated are shown in Fig. 2a (upper plot). The bottom plot of Fig. 2a represents the ΔT signal and the 5 truncation times ($t_1 ... t_5$). The corresponding $\Delta\phi$ plots ($\Delta\phi_1 .. \Delta\phi_5$) obtained from the data set of Fig. 2a for these observation intervals are in Fig. 2b. Time t_4 corresponds roughly to ΔT duration and therefore $\Delta\phi_4$ is considered a good $\Delta\phi$ profile. In fact, with respect to $\Delta\phi_4$, curves $\Delta\phi_1$, $\Delta\phi_2$, and $\Delta\phi_3$ are distorted while $\Delta\phi_5$ does not show an appreciable improvement despite its higher frequency resolution (in this case double).

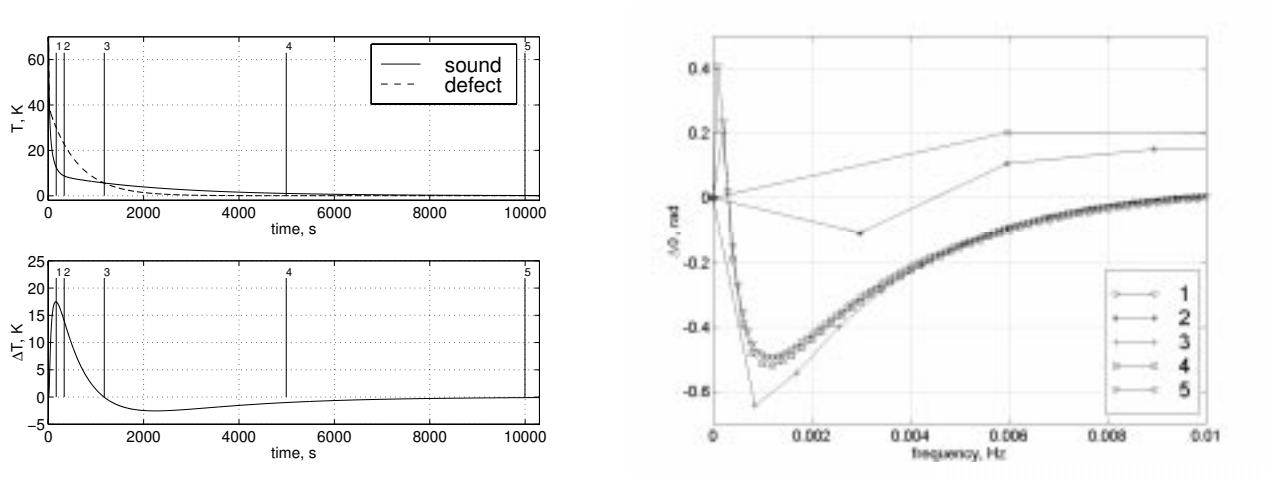

(a) *(b)*

Figure 2. Temperature and thermal contrast evolution curves (a) and the phase difference for different observation times (b).

It is worth noting that also $\Delta\phi_3$ could be taken as a good profile when considering its shape. However, it is difficult to determine exactly when the maximum phase shift occurs due to the poor frequency resolution. Moreover, this maximum occurs at the first resolved frequency and therefore signals at lower frequencies (deeper defects) are unresolvable.

In conclusion, the observation interval should begin before the appearance of any defect signal and end after all the thermal contrast signals become negligible. This is well illustrated in Fig. 3. Temperature evolution and relative thermal contrast signals for three defects at different depth are represented in Fig. 3a. The corresponding $\Delta\phi$ profiles for two different observation periods are shown in Fig. 3b, respectively upper and lower plots. For the shallowest defect (defect 1), the thermal contrast signal is significantly decreased by the end of both observation periods, and therefore both observation times give similar, both in shape and magnitude, phase difference profiles. For the deeper defects (defects 2 and 3), the thermal contrast signals are significantly longer than the shortest observation time, but not the longer one. Therefore, there is a significant change in the phase difference profiles, due to insufficient frequency resolution for the shorter duration observation time.

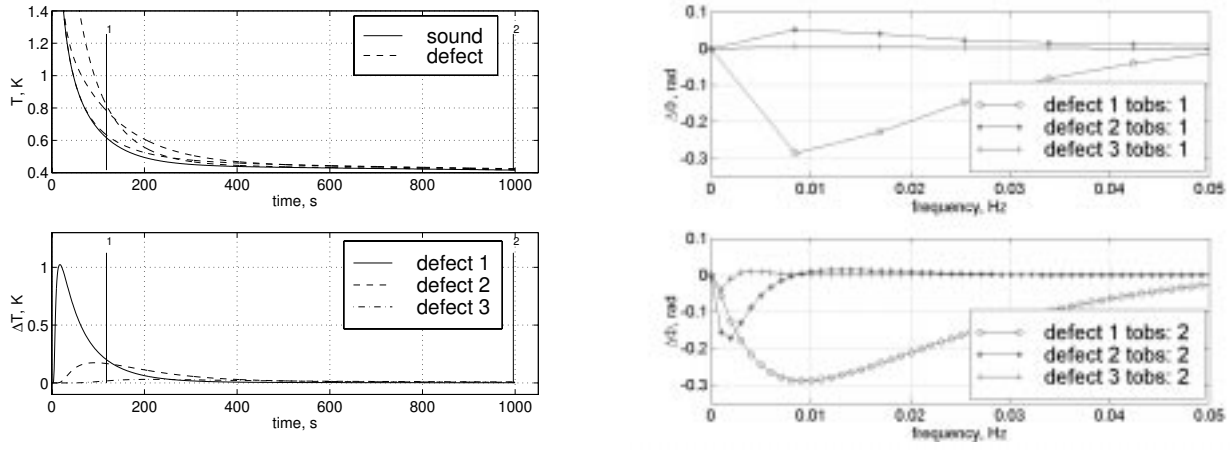

(a) *(b)*

Figure 3. Temperature and thermal contrast evolution profiles (a) and phase difference for two different observation periods (b).

5. SAMPLING RATE

The other essential parameter in DFT is the sampling frequency because it is directly related to the aliasing error. Aliasing error distorts the frequency spectrum (and therefore the phase). It is well known that for bandwidth-limited signals, in order to eliminate the aliasing error, the sampling frequency should be greater than the Nyquist frequency

$$f_N \geq 2 \cdot B \ . \tag{4}$$

If the signal has *"in practice"* limited bandwidth, aliasing error can still be maintained at acceptable levels by means of oversampling methods[5], resulting in no significant distortion of the frequency spectrum.

For defect detection by means of PPT, the phase difference is sought between defect and sound zones. Therefore, sampling frequency has to be chosen in order to accurately determine the phase difference. The main problem then becomes: what is the lowest sampling frequency required to accurately determine the phase difference? This requires determining the contribution of aliased frequencies on the highest frequency of interest.

It can be argued that some parameter extracted from the shape of ΔT signal could help in the identification of this frequency (i.e. rise time, etc.). However, this does not yield accurate results since the ΔT shape is influenced by the workpiece itself (relative depth of defect with respect to sound zone, 2D and 3D effects depending on the defect and specimen geometries) and by the boundary conditions (heating pulse shape, convective fluxes, etc.). Sampling frequency has therefore to be examined experimentally with the aim of obtaining an accurate phase difference.

Fig. 4a contains the ΔT signal of a single defect sampled at 4 different frequencies: 0.01, 0.1, 0.5, and 1.5 Hz. The corresponding $\Delta\phi$ distributions in frequency domain are shown in Fig. 4b together with the analytical $\Delta\phi$ profile (solid line curve). The differences between $\Delta\phi$ signals are due to aliasing error. This is shown very clearly on the 0.01 Hz plot where the sampling frequency is very close to the frequency range of interest.

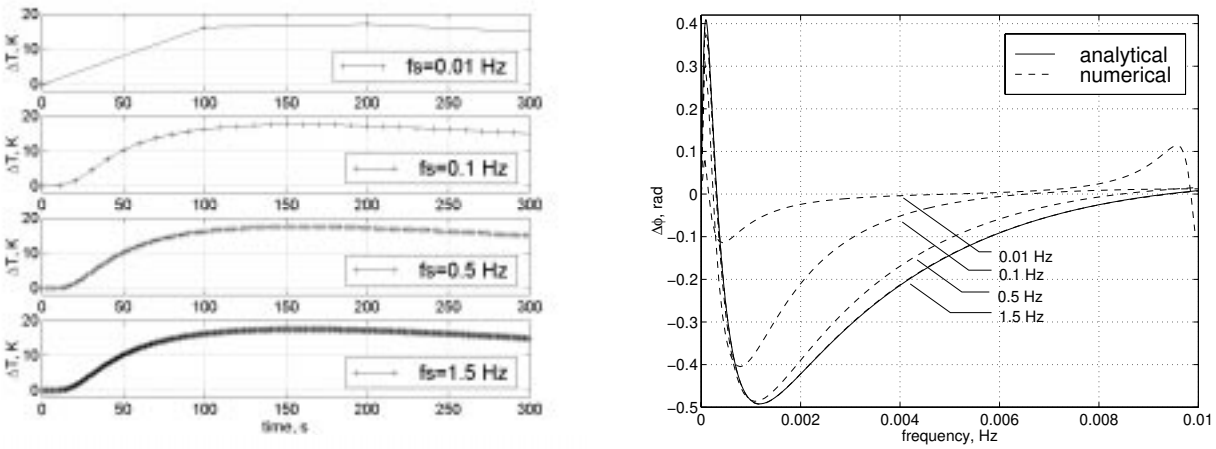

(a) *(b)*

Figure 4. Thermal contrast evolution (a) and the corresponding phase difference plots (b) obtained for different sampling rates.

Aliasing error increases with decreasing sampling frequencies: the aliasing errors are negligible at f_s*=1.5 Hz* and at f_s*=0.5 Hz*, and they gain importance at f_s*=0.1 Hz* and f_s *= 0.01 Hz*. It is worth noting however that the distortion of $\Delta\phi$ due to aliasing error is not proportional to sampling frequency but instead is negligible for high sampling frequencies and increases abruptly for very low sampling frequencies.

Fig. 5a shows the $\Delta\phi$ and ϕ loss at various sampling frequencies with respect to the analytical (continuous) signal. The $\Delta\phi$ graph shows that as the sampling rate decreases below the knee, the attenuation increases dramatically. As a practical conclusion, accurate phase difference measurements are realized if the sampling frequency is greater than the knee in the attenuation curve.

6. INFLUENCE OF 3D EFFECTS ON $\delta\phi$

Finite lateral defect size makes defect visualization in thermography much more complicated. Three-dimensional heat

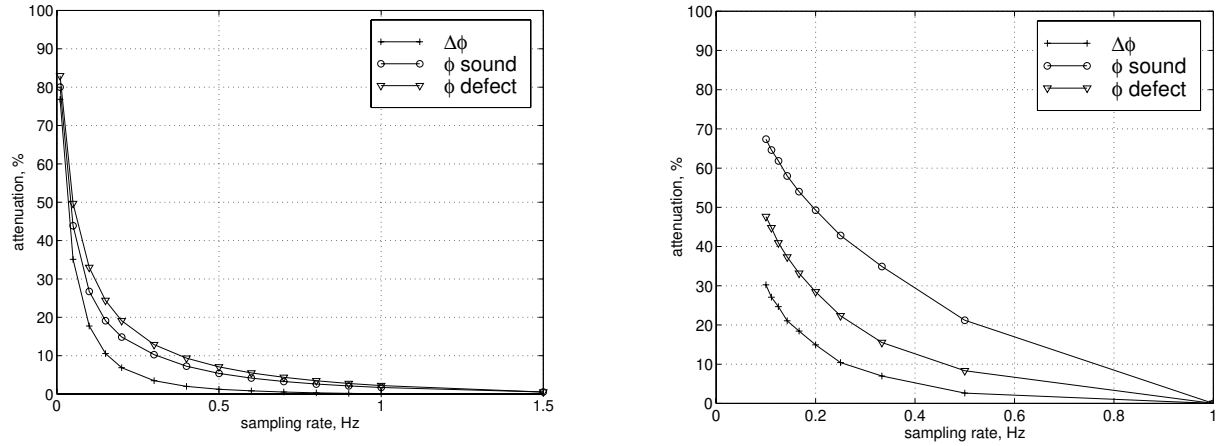

Figure 5. Sampling rate influence on the phase difference. a) simulated; b) experimental.

diffusion around a defect decreases thermal contrast on the surface. To investigate the influence of the defect lateral size on the phase difference, a 3D finite difference model, described in details elsewhere[6], is used. The thermally insulated plate of thickness 20 mm ($\alpha=4\cdot10^{-7}\ m^2s^{-1}$) with a square open-bottom defect located 10 mm below the surface is considered. The size l of the defect is varied while the depth is having the same value. In Fig. 6 the phase difference profiles obtained for variable defect size l^* normalized by the defect depth are shown. The simulated temperature signals above the defect center and in the sound area are used to compute the phase difference.

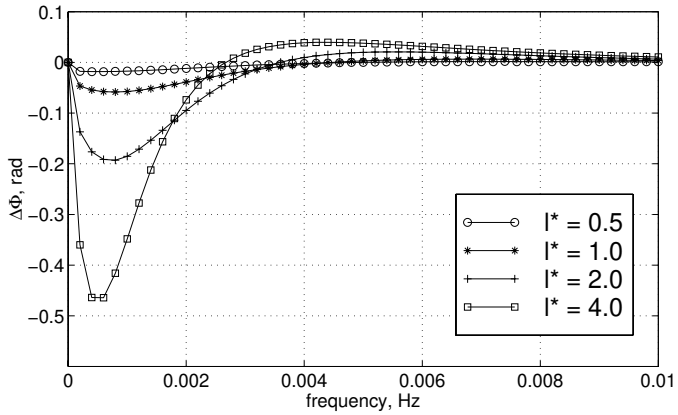

Figure 6. The influence of the normalized defect size on the phase difference.

The defect is well-recognized on the phase difference profile when its size is in two times bigger than its depth. It is detect able when its size is approximately its depth, but for the size less than a half of the depth it is likely to be undetectable for experimentally obtained noisy phase image.

7. EXPERIMENTAL RESULTS

To experimentally verify the guidelines for collecting data for PPT analysis, measurements were performed on two specimens. The first sample is a 25 mm thick piece of opaque plastic with several flat bottom holes in it. The artificial voids are square shaped having 25 mm on a side. They are located under the observed surface at a variable depth. Two flash lamps producing 6 KJ pulse for duration of 10 ms are used to excite the surface. The thermal response is collected radiatively by an

infrared focal plane array camera. A series of 1000 digitized images having 256 x 256 pixels with 12 bit resolution collected by the camera with a sampling rate of 1 Hz is transferred into a personal computer.

The DFT is performed on measured time responses of a sound region and regions over the voids located at depths of 1.6, 3.2, 4.8, 6.4 mm below the surface. Phase plots are represented in Fig. 7a and corresponding $\Delta\phi$ plots in Fig. 7b. It is clear, that relationship between $\Delta\phi$ and the defect depth is in good agreement with the one obtained with the analytical model (Fig. 3b). The phase maps (phasegrams) computed for frequencies 0.001, 0.002, 0.004, 0.006, and 0.008 Hz are shown in Fig. 8a.

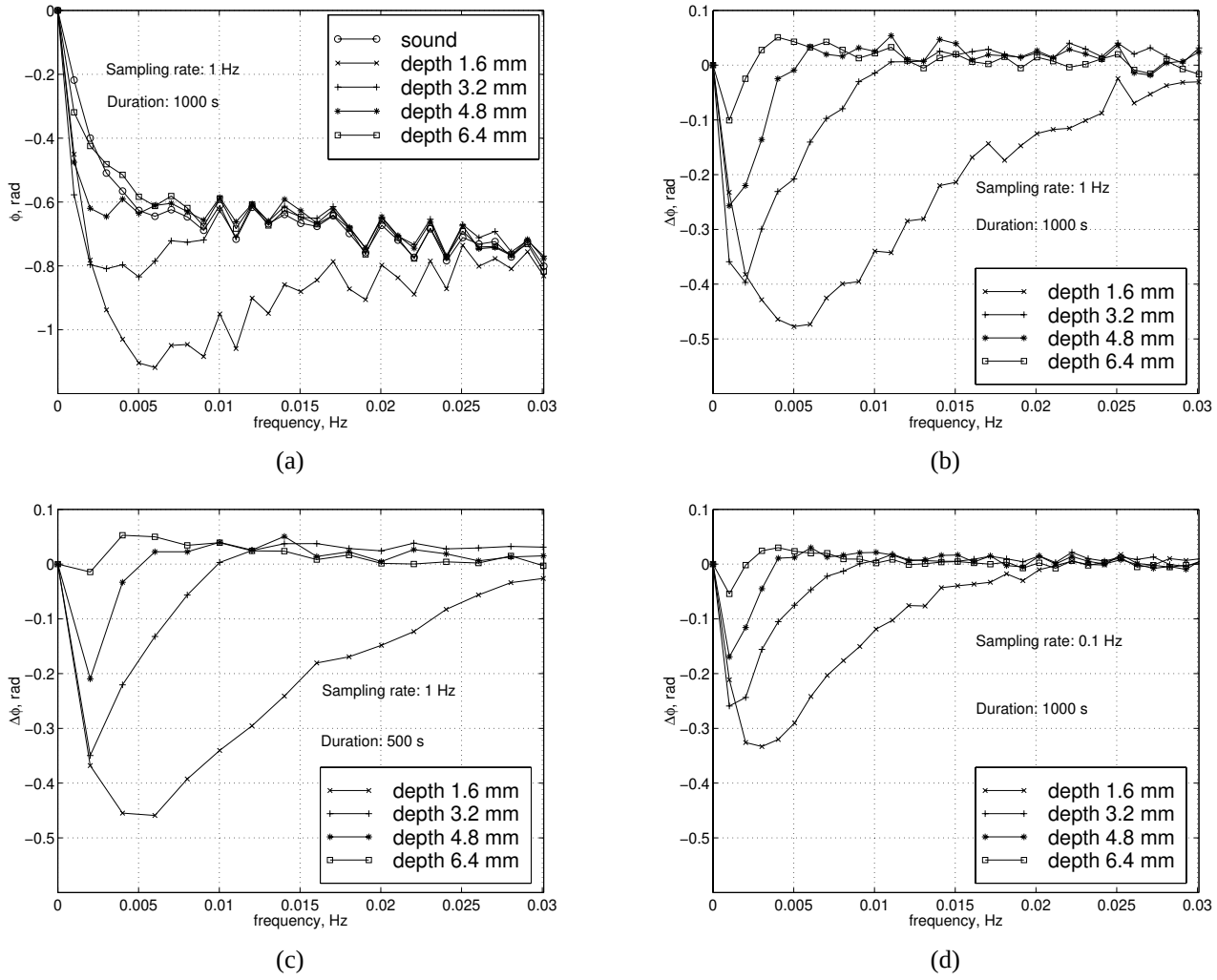

Figure 7. Phase (a) and phase difference (b-d) profiles as function of frequency obtained on the plastic specimen with the flat bottom holes.

In order to evaluate the truncation and aliasing errors introduced by incorrect parameter selection (observation period and sampling frequency), the same sequence has been truncated to 500 s and undersampled (0.1 Hz). Corresponding $\Delta\phi$ plots are shown in Fig. 7c and 7d. It is worth noting that in Fig. 7c the frequency sample at 0.001Hz is not resolved and therefore the deepest defect is not visible any more due to truncation error. Fig. 8b shows the phasegrams obtained from the truncated sequence. Phasegram at 0.001Hz is missing because this frequency sample is unresolved and the deepest defect is not visible. Phasegrams related to higher frequency samples are almost not influenced by truncation error. On the other hand, in Fig. 7d $\Delta\phi$ profiles show a distortion (lower magnitude) due to aliasing error introduced by undersampling. Fig. 8c shows the phasegrams obtained from the undersampled sequence. The distortion is more visible at high frequency samples while at low frequencies it is almost negligible and all 4 defects are visible.

The phase analysis enables detection of holes deep in the specimen (in our case - up to 7 mm). The in-depth scanning

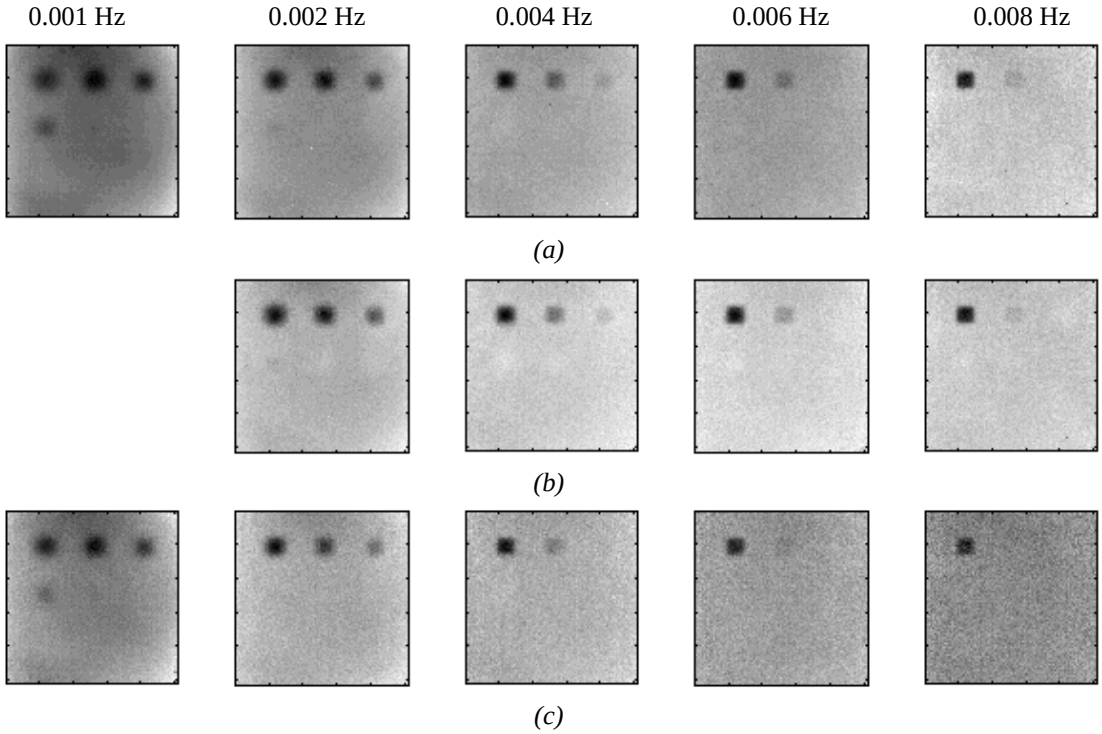

Figure 8. Phasegrams of the plastic panel. a) f_s=*1 Hz*, t_{obs}=*1000 s*; b) f_s=*1 Hz*, t_{obs}=*500 s*; c) f_s=*0.1 Hz*, t_{obs}=*1000 s*.

capability reported earlier[1,2] is presented in Fig. 8. The longer the observation time (the lower frequency) the deeper the defects that can be viewed. Moreover, the deeper the defect, the lower its signal and the less high frequency content. The deepest defect is visible just in the first image (Fig. 8a and 8c) while the shallowest one (located at the top-left corner) shows a very strong signal and its contribution lasts for a wider range of frequencies.

The attenuation of the $\Delta\phi$ signal for the deepest defect as a function of the sampling rate has been analyzed (Fig. 5b). The

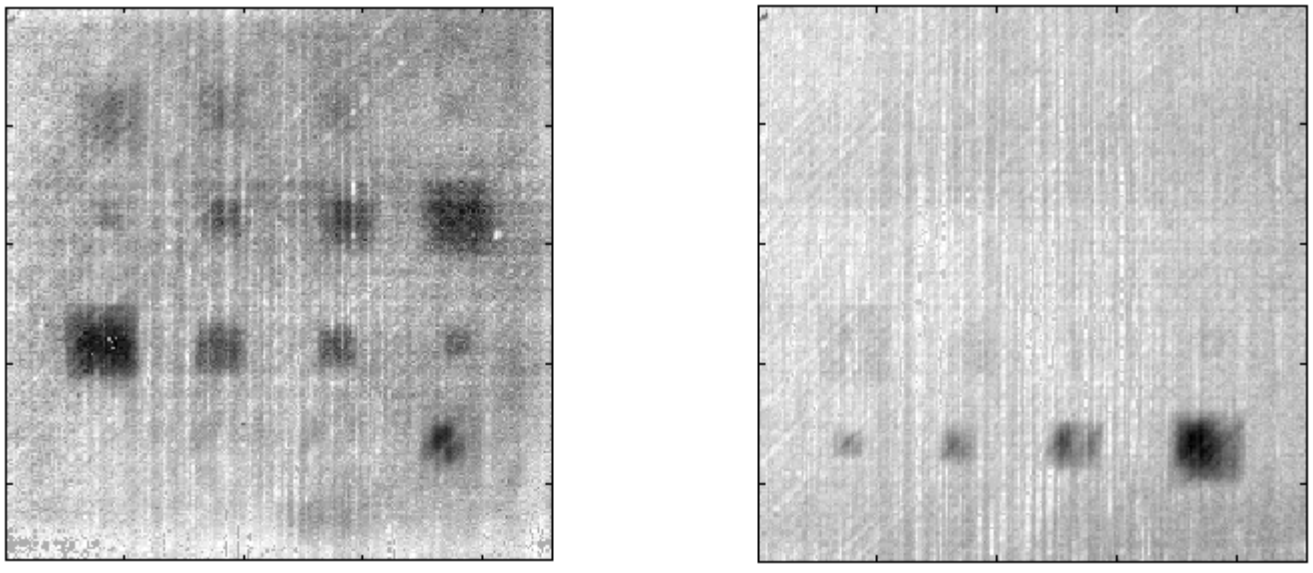

Figure 9. Phasegrams of a CFRP panel with inclusions of different size and depth. f_s=*30 Hz*; t_{obs}=*16 s*. a) harmonic 1 (0.06 Hz); b) harmonic 7 (0.44 Hz).

result is that a rate of 0.5 Hz introduces an attenuation $\Delta\phi$ of just 2.5% with the advantage of reducing the data acquisition requirements from 1000 images to 500 images.

The second specimen is a piece of 20-ply CFRP with artificial inclusions of different size and depth. It has been fabricated to explore the detectability limits of the thermographic inspection of the aerospace composite structures. A doubled 25 micron Nylon® bagging film has been inserted into the laminate to represent delaminations between plies. The inserts are located in four rows under 2^{nd}, 5^{th}, 8^{th}, and 10^{th} plies. Each row consists of four squares which are 13, 19, 25, and 38 mm on a side. The data set collected on this sample contains 500 images with a sampling rate of 30 Hz.

The computed phasegrams are shown in Fig. 9. The phasegrams provide information about the defects which can be effectively employed for defect edge extraction[7]. Unfortunately, phase images at two different frequencies are required to visualize all of the flows in the specimen.

8. SUMMARY

This study has been done to establish general guidelines for the data acquisition process for PPT. The parameters of interest are the duration of the observation period and the sampling rate during the observation. While the data processing based on the thermal contrast usually requires an achievement of its maximum, the time interval of PPT measurement should extend from the appearance of the defect under investigation and last until its contrast is negligible. Often it is possible to decrease the sampling rate during the thermal data collection without significant loss of quality in the phase difference image. Follow definition of an acceptable phase difference loss, the lowest sampling rate can be determined from the attenuation curve.

ACKNOWLEDGMENTS

This work was performed while author Plotnikov held a National Research Council - NASA Langley Research Center Research Associateship.

REFERENCES

1. X. Maldague, S. Marinetti, “Pulse Phase Infrared Thermography”, *J. Appl. Phys.*, 79 (5), pp. 2694-2698, 1996.
2. X. Maldague, S. Marinetti, J.P. Couturier, “Applications of Pulse Phase Thermography”, in: *Review of Progress in QNDE,* D.O. Thompson and D.E. Chimenti (Eds.), Vol. 16A, pp. 339-344, Plenum Press, N.Y., 1997.
3. X. Maldague, J.-P. Couturier, S. Marinetti, A. Salerno, D. Wu, “Advances in Pulsed Phase Thermography”, in: *Quantitative Infrared Thermography QIRT 96,* Proc. of Eurotherm SEMINAR 50, pp. 377-382, Ed. ETS, Stuttgart (Germany), 1996.
4. K. Beauchamp, C. Yuen, *Digital Methods for Signal Analysis*, George Allen & Unwin, London, 1979.
5. R. E. Crochiere, L. R. Rabiner, “Multirate Processing of Digital Signals”, in: *Advanced Topics in Signal Processing*, J. S. Lim and A. V. Oppenheim (Eds.), Prentice Hall, Englewood Cliffs, NJ, 1988.
6. Y.A. Plotnikov, W. P. Winfree, Thermographic Imaging of Defects in Anisotropic Composites, in: *Review of Progress in QNDE,* D.O. Thompson and D.E. Chimenti (Eds.), Vol. 17A, pp. 457-464, Plenum Press, N.Y., 1998.
7. Y.A. Plotnikov, W.P. Winfree, “Advanced Image Processing for Defect Visualization in Infrared Thermography”, in: *Thermosense XX*, J.R. Snell , Jr. and R.N. Wurzbach, (Eds.), SPIE Vol. 3361, pp. 331-338, SPIE, Bellingham, WA, 1998.